Effect of Matrix Aging on the Behavior of Human Serum Albumin Entrapped in a Tetraethyl Orthosilicate-Derived Glass

Kulwinder K. Flora and John D. Brennan*

Department of Chemistry, McMaster University, Hamilton, Ontario L8S 4M1, Canada

Received February 22, 2001. Revised Manuscript Received July 31, 2001

The steady-state and time-resolved fluorescence of Trp-214 was used to examine the conformation, dynamics, accessibility, thermal stability, and degree of ligand binding of human serum albumin (HSA) after entrapment of the protein in sol−gel processed glasses. The bioglasses were derived from tetraethyl orthosilicate and were aged in air without washing (dry-aged), in air after a washing step (washed), or in buffer (wet-aged). In all cases, significant changes were observed in the structure and dynamics of HSA, consistent with adsorption of the protein onto the silica surface combined with partial unfolding of the protein. Significant changes in the thermal stability and degree of ligand binding of the entrapped protein were also observed, with both stability and ligand binding capacity decreasing as aging continued. All proteins showed full accessibility to neutral quenchers over 2 months of aging but only partial accessibility to negatively charged quenchers, even at early aging times, indicating electrostatic repulsion of such analytes by the negatively charged matrix. Taken together, the results indicated that the reduced ligand binding for entrapped HSA was caused by a combination of protein denaturation and partial inaccessibility of the protein to negatively charged species. After 2 months of aging the entrapped proteins retained less than 15% of their binding ability in solution, regardless of which method was used to age the material. In light of these results, it is clear that improved sol−gel processing methods will be needed to overcome the time-dependent changes in the structure and function of proteins entrapped in silicate-based glasses.

Introduction

The characteristics of proteins entrapped in glasses formed by the sol−gel processing method have been studied extensively in the past few years. Numerous reports have appeared describing the function,[1] structure,[2] dynamics,[3] accessibility,[2,4] reaction kinetics,[2a,5] initial stability,[6] and long-term stability[7] of entrapped proteins. However, only a few reports have considered how these factors are influenced by the methods used for matrix aging and the length of time that the matrix has aged. For example, Bright and co-workers have shown that the dynamics of acrylodan-labeled human serum albumin (HSA) and bovine serum albumin (BSA) decreased as sol−gel processed glasses aged.[3a] However, the effect of different aging methods was not addressed in this work, and no correlation to protein function was done. Saavedra et al. have shown that the conformational flexibility and accessibility of entrapped BSA decreased in glasses that were aged in air[4] or in buffer[2c] for 1 week. However, no results were given for how these parameters changed as aging progressed, and again the

* To whom correspondence should be addressed. Phone: 905-525-9140 (ext. 27033). Fax: 905-522-2509. E-mail: brennanj@mcmaster.ca.

(1) (a) Brennan, J. D. *Appl. Spectrosc.* **1999**, *53*, 106A. (b) Braun, S.; Shtelzer, S.; Rappoport, S.; Avnir, D.; Ottolenghi, M. *J. Non-Cryst. Solids* **1992**, *147*, 739. (c) Avnir, D.; Braun, S.; Lev, O.; Ottolenghi, M. *Chem. Mater.* **1994**, *6*, 1605. (d) Wang, R.; Narang, U.; Prasad, P. N.; Bright, F. V. *Anal. Chem.* **1993**, *65*, 2671. (e) Ellerby, L. M.; Nishida, C. R.; Nishida, F.; Yamanaka, S. A.; Dunn, B.; Valentine, J. S.; Zink, J. I. *Science* **1992**, *225*, 1113. (f) Wu, S.; Ellerby, L. M.; Cohan, J. S.; Dunn, B.; El-Sayed, M. A.; Valentine, J. S.; Zink, J. I. *Chem. Mater.* **1993**, *5*, 115. (g) Dave, B. C.; Soyez, H.; Miller, J. M.; Dunn, B.; Valentine, J. S.; Zink, J. I. *Chem. Mater.* **1995**, *7*, 1431. (h) Yamanaka, S. A.; Nishida, F.; Ellerby, L. M.; Nishida, C. R.; Dunn, B.; Valentine, J. S.; Zink, J. I. *Chem. Mater.* **1992**, *4*, 495. (i) Dave, B. C.; Dunn, B.; Valentine, J. S.; Zink, J. I. *Anal. Chem.* **1994**, *66*, 1120A. (j) Blyth, D. J.; Aylott, J. W.; Richardson, D. J.; Russell, D. A. *Analyst* **1995**, *120*, 2725. (k) Aylott, J. W.; Richardson, D. J.; Russell, D. A. *Analyst* **1997**, *122*, 77. (l) Williams, A. K.; Hupp, J. T. *J. Am. Chem. Soc.* **1998**, *120*, 4366−4371.

(2) (a) Zheng, L.; Reid, W. R.; Brennan, J. D. *Anal. Chem.* **1997**, *69*, 3940. (b) Zheng, L.; Brennan, J. D. *Analyst* **1998**, *123*, 1735. (c) Edmiston, P. L.; Wambolt, C. L.; Smith, M. K.; Saavedra, S. S. *J. Colloid Int. Sci.* **1994**, *163*, 395.

(3) (a) Jordan, J. D.; Dunbar, R. A.; Bright, F. V. *Anal. Chem.* **1995**, *67*, 7, 2436−43. (b) Gottfried. D. S.; Kagan, A.; Hoffman, B. M.; Friedman, J. M. *J. Phys. Chem. B* **1999**, *103*, 2803−2807. (c) Doody, M. A.; Baker, G. A.; Pandey, S.; Bright, F. V. *Chem. Mater.* **2000**, *12*, 1142−1147.

(4) Wambolt, C. L.; Saavedra, S. S. *J. Sol-Gel Sci. Technol.* **1996**, *7*, 53−57.

(5) Shen, C.; Kostic, N. M. *J. Am. Chem. Soc.* **1997**, *119*, 1304−1312.

(6) (a) Braun S.; Rappoport, S.; Zusman, R.; Avnir, D.; Ottolenghi, M. *Mater. Lett.* **1990**, *10*, 1−5. (b) Heichal-Segal, O.; Rappoport, S.; Braun, S. *Biotechnology* **1995**, *13*, 798−800. (c) Reetz, M. T.; Zonta, A.; Simpelkamp, J. *Biotechnol. Bioeng.* **1996**, *49*, 527−534. (d) Keeling-Tucker, T.; Rakic, M.; Spong, C.; Brennan, J. D. *Chem. Mater.* **2000**, *12*, 3695.

(7) (a) Narang, U.; Prasad, P. N.; Bright, F. V.; Kumar, K.; Kumar, N. D.; Malhotra, B. D.; Kamalasanan, M. N.; Chandra, S. *Chem. Mater.* **1994**, *6*, 1596−1598. (b) Narang, U.; Prasad, P. N.; Bright, F. V.; Ramanathan, K.; Kumar, N. D.; Malhotra, B. D.; Kamalasanan, M. N.; Chandra, S. *Anal. Chem.* **1994**, *66*, 3139−44. (c) Jordan, J. D.; Dunbar, R. A.; Bright, F. V. *Anal. Chim. Acta* **1996**, *332*, 83−91. (d) Yamanaka, S. A.; Dunn, B.; Valentine, J. S.; Zink, J. I. *J. Am. Chem. Soc.* **1995**, *117*, 9095−96. (e) Kauffmann, C.; Mandelbaum, R. T. *J. Biotechnol.* **1998**, *62*, 169−176.

10.1021/cm010155l CCC: $20.00
Published on Web 09/25/2001

results were not correlated to changes in protein function. Our group has shown that matrix aging can alter the function of entrapped proteins, with the binding affinity of entrapped Ca^{2+} binding proteins such as parvalbumin[8] and oncomodulin[9] decreasing as aging proceeds owing to alterations in electrostatic interactions between the protein and the matrix.

It is well-known that the evolution of a sol−gel-derived material is dependent on the storage conditions employed after gelation (aging), the time over which aging is done, and the degree to which the material is allowed to dry. As aging progresses, cross-linking of the network increases and the internal solvent is expelled from the matrix, causing the internal polarity and viscosity to change and the average pore size to decrease in a manner that depends on the aging conditions.[10,11] If aging is done for a relatively long period and is combined with partial drying, average pore diameters within the silicate matrix can decrease to values less than 10 nm,[10,12] and in such cases solvent loss may cause entrapped species to become inaccessible[2,4] or adsorb to the silica surface.[3b] Given the intimate relationship between the local microenvironment and the conformation and function of a protein, one might expect aging of a bioglass to produce dramatic changes in the behavior of an entrapped protein.[1a]

The usefulness of an entrapped protein is determined primarily by its ability to bind to external analytes that enter the matrix and thereby catalyze a reaction or generate an analytical signal and, thus, is related to the overall function of the protein. The ability of an entrapped protein to bind an analyte requires that the protein be accessible to analyte, be in a native form so that it can bind analyte, and be able to undergo any necessary conformational changes upon binding of analyte to produce a desired reaction or signal.[8,13] To examine these issues, we have monitored the behavior of HSA as a function of time after entrapment into sol−gel-derived silicate matrixes that were aged in air without washing (dry-aged), in air with an initial washing step (washed), or in buffer (wet-aged). HSA was chosen because it is relatively large and complex (MW of 60 kDa with 3 major domains[14]) but yet contains only a single Trp residue within the protein at position 214 in domain II,[15] allowing for detailed fluorescence studies. HSA was also chosen because its behavior has been well characterized in solution[16] and because it allows comparisons with previous studies of entrapped HSA and BSA.[2c,3a,4] In the present work, the steady-state and time-resolved fluorescence of the single Trp residue was used to provide information on the conformation, dynamics, thermal stability, accessibility, and ligand-binding properties of HSA when entrapped in tetraethyl orthosilicate-derived materials. The changes in these parameters are followed as a function of aging time and conditions and show that the ligand-binding capacity of the protein changes with time as a result of changes in both protein denaturation and accessibility to analytes.

Experimental Section

Chemicals. Human serum albumin (HSA, essentially fatty acid free), salicylic acid, and polymethacrylate fluorometer cuvettes (transmittance curve C) were obtained from Sigma (St. Louis, MO). Tetraethyl orthosilicate (TEOS, 99.999+%), potassium iodide (99.9%), and acrylamide (99+%) were supplied by Aldrich (Milwaukee, WI). Guanidine hydrochloride (GdHCl, Sequanol grade) was obtained from Pierce (Rockford, IL). Sephadex G-25 fine powder was supplied by Pharmacia Biotech (Uppsala, Sweden). All water was twice distilled and deionized to a specific resistance of at least 18 MΩ·cm. All other chemicals were of analytical grade and were used without further purification.

Procedures. *Entrapment of Protein.* HSA was first purified as described elsewhere[15a] and diluted into phosphate-buffered saline (PBS; 10 mM phosphate buffer, 100 mM KCl, pH 7.2) to a concentration of 20 μM, as determined using $\epsilon_{277} = 36\,000$ M^{-1} cm^{-1} for HSA.[16d] Sols were prepared by sonicating a mixture of 4.5 mL of TEOS, 1.4 mL of water, and 100 μL of 0.1 N HCl for 1 h at ambient temperature until the mixture became clear, colorless, and monophasic. The solution was then cooled and kept in the freezer at −20 °C for 7−10 days before the addition of protein. Sol−gel matrixes were prepared in the form of blocks (1.5 cm × 1 cm × 1 cm) by mixing 0.75 mL of the sol with 0.75 mL of the protein solution. Blocks were utilized in the current study to eliminate scattering artifacts, which were observed using thin sol−gel slides (described in ref 2a), and to allow studies of samples at very early aging times, when thin slides were too soft to mount reproducibly. All samples were aged at 4 °C using three different methods. The wet-aged and washed samples were immediately filled with 2 mL of 10 mM phosphate buffer after gelation and allowed to stand overnight at 4 °C, whereas the dry-aged samples had no buffer added at any stage. Wet-aged and washed blocks were rinsed for 10 min two more times to exchange residual ethanol with buffer. Previous studies using the ethanol-sensitive fluorescent dye pyranine indicated that such a washing procedure was sufficient to remove all the entrapped ethanol.[12] After rinsing, the washed blocks were aged in air while the wet-aged blocks were aged in the presence of the wash buffer for the duration of aging. Wet-aged samples were tested in the presence of fresh buffer to eliminate any possibility of fluorescence signals from contaminants in the wash buffer.

Steady-State Fluorescence Measurements. Fluorescence measurements were performed using a SLM 8100 spectrofluorimeter (Spectronic Instruments, Rochester, NY), as described elsewhere.[1a] HSA emission spectra were excited at 295 nm with emission collected from 305 to 450 nm. All spectra were collected in 1 nm increments using 4 nm band-passes on the excitation and emission monochromators and an integration time of 0.3 s/point. Appropriate blanks were subtracted from each sample, and the spectra were corrected for the wavelength dependence of the emission monochromator throughput and detector response.

(8) Flora, K. K.; Brennan, J. D. *Anal. Chem.* **1998**, *70*, 4505.
(9) Zheng, L.; Flora, K. K.; Brennan, J. D. *Chem. Mater.* **1998**, *10*, 3974.
(10) Brinker, C. J.; Scherer, G. W. *Sol−Gel Science: The Physics and Chemistry of Sol−Gel Processing;* Academic Press: San Diego, CA, 1990.
(11) Dunn, B.; Zink, J. I. *Chem. Mater.* **1997**, *9*, 2280.
(12) Flora, K. K.; Dabrowski, M. A.; Musson, S. P. Brennan, J. D. *Can. J. Chem.* **1999**, *77*, 1617.
(13) (a) Brennan, J. D.; Flora, K. K.; Bendiak, G.; Baker, G. A.; Kane, M.; Pandey, S.; Bright, F. V. *J. Phys. Chem. B* **2000**, *104*, 10100. (b) Brennan, J. D. *J. Fluoresc.* **1999**, *9*, 295.
(14) Carter, D. C.; Ho, J. X. *Adv. Protein Chem.* **1994**, *45*, 153.
(15) Brown, J. R. In *Albumin Structure, Function and Uses*; Rosenoer, V. M., Oratz, M., Rothschild, M. A., Eds.; Pergamon: Oxford, U.K., 1977; pp 27−51.
(16) (a) Flora, K. K.; Brennan, J. D.; Baker, G. A.; Doody, M. A.; Bright, F. V. *Biophys. J.* **1998**, *75*, 1084. (b) Pico, G. A. *Biochem. Mol. Biol. Int.* **1995**, *36*, 1017. (c) Pico, G. A. *Biochem. Mol. Biol. Int.* **1996**, *38*, 1. (d) Pico, G. A. *Int. J. Biol. Macromol.* **1997**, *20*, 63. (e) Wetzel, R.; Becker, M.; Behlke, J.; White, H.; Bohn, S.; Ebert, B.; Hamaann, H.; Krumbiegel, J.; Lasiman, G. *Eur. J. Biochem.* **1980**, *104*, 469. (f) Lee, J. Y.; Hirose, M. *J. Biol. Chem.* **1992**, *267*, 14753. (g) Farruggia, B.; Gabriela, G.; D'Angelo C.; Pico, G. *Int. J. Macromol.* **1997**, *20*, 43. (h) Narazaki, R.; Maruyama, T.; Otagiri, M. *Biochim. Biophys. Acta* **1997**, *1338*, 275.

Steady-state fluorescence anisotropy measurements were performed in the L-format using Glan-Taylor prism polarizers in the excitation and emission paths, as described previously.[1a] Single point fluorescence anisotropy measurements were generally made at the maximum emission wavelength, using excitation at 295 nm. Band-passes of 8 nm were used in the excitation and emission paths, with the signal integrated for 3 s. All fluorescence anisotropy values were corrected for the instrumental *G* factor to account for any polarization bias in the monochromators. All fluorescence anisotropy values reported were the average of 5 measurements each on three different samples. Steady-state anisotropy values were converted to average rotational reorientation times (ϕ_{SS}) using the following equation:

$$r = \frac{r_0}{1 + (\langle\tau\rangle/\phi_{SS})} \quad (1)$$

Here r is the measured fluorescence anisotropy, r_0 is the limiting anisotropy, and $\langle\tau\rangle$ is the intensity-weighted mean fluorescence lifetime of the sample as determined using eq 4 below. A limiting anisotropy of 0.310 ± 0.003 (λ_{ex} = 295 nm) was used for the tryptophan residue of HSA.[17]

Time-Resolved Fluorescence. Time-resolved fluorescence intensity decay data were acquired in the time domain using a PTI laserstrobe fluorimeter (Photon Technologies Incorporated, London, ON, Canada), as described elsewhere.[13a,18] Samples were excited at 295 nm with emission collected under magic angle polarization conditions and passed through a monochromator (4 nm band-pass) set at 335 nm. The intensity data was collected into 25 ps time windows, starting 2 ns before the laser pulse arrived (to establish a prepulse baseline) and covering a 40 ns range. The instrument response function was collected by measuring the Rayleigh scattering of the laser pulse from water and was used to deconvolute the instrument response profile from the experimentally determined decay trace. Appropriate baseline offset and time-shift parameters were obtained by allowing these to be floating parameters in the fit.

The function describing the fluorescence intensity decay was fit using a global analysis method to both discrete and distributed fitting models, with goodness-of-fit evaluated using the reduced χ^2 parameter, residual plots, and autocorrelation plots.[19] In all cases, the best fit to the decay data was obtained using a sum of discrete exponential components, given by

$$I(t) = \sum_i \alpha_i \exp(-t/\tau_i) \quad (2)$$

where τ_i is the decay time and α_i is the preexponential factor of the ith decay component. The fractional fluorescence of component i (f_i) was calculated from

$$f_i = \alpha_i\tau_i / \sum_i \alpha_i\tau_i \quad (3)$$

Using global analysis, the lifetime components were linked for each sample and thus remained fixed as a function of aging, while the fractional proportion of each lifetime component was allowed to vary as the samples aged. Fractional fluorescence values were also used to calculate the intensity-weighted mean lifetime values from the following equation:

$$\langle\tau\rangle = \sum_i f_i\tau_i \quad (4)$$

Time-resolved decays of fluorescence anisotropy were constructed from intensity decays that were obtained using vertically polarized excitation and vertically polarized emission (I_{VV}) or horizontally polarized emission (I_{VH}) and were corrected for the instrument response profile and the instrumental *G* factor, as described in detail elsewhere.[20] The anisotropy decay was fit to a two-component hindered rotor model according to the following equation:

$$r(t) = (r_0 - r_\infty)[\beta_1 \exp(-t/\phi_1) + \beta_2 \exp(-t/\phi_2)] + r_\infty \quad (5)$$

Here ϕ_1 reflects slow rotational motions associated rotation of the entire protein (global motion), ϕ_2 reflects rapid rotational reorientation of Trp residue around its bond axis (local motion), and r_∞ is the residual anisotropy of the protein at long times that reflects hindered rotation of the protein. The terms β_1 and β_2 represent the fractional contributions to the total anisotropy decay from the slow and fast motions, respectively ($\Sigma\beta_i = 1$).[20] The goodness-of-fit was evaluated by minimizing the sum-of-squares of residuals (SSR) between the line-of-best-fit and the experimental decay trace and by the randomness of residual plots and autocorrelation plots. The SSR was typically less than 1×10^{-5} for satisfactory fits. All fluorescence lifetime and anisotropy decay values reported are the average over three different samples.

Thermal Denaturation Studies. Fluorescence-based thermal denaturation studies of entrapped HSA were done as described previously.[2b,16a] The integrated emission intensity was plotted against sample temperature and the midpoint of the resulting unfolding curve was determined by nonlinear fitting to extract unfolding temperatures (T_{un}). An equilibration time of 20 min was allowed at each temperature before emission spectra were collected. This equilibration time was found to be sufficient as the signal did not change when using longer equilibration times. Cooling the samples indicated that the unfolding transition was not reversible (in agreement with studies of HSA denaturation in solution[16a]); thus, thermodynamic parameters related to the protein unfolding event could not be obtained.[2b,16a]

Salicylate Titrations of HSA. The dimensions of blocks were such that titrations required several hours per point to complete, since salicylate and the sol−gel matrix are both negatively charged. For this reason, measurements were done only at a 1.75:1 molar ratio of salicylate:protein. Fluorescence lifetimes were measured with excitation at 295 nm and emission at 480 nm (salicylate fluorescence), and the data were fit to a discrete decay model. The ratios of preexponential factors for the lifetimes of free and bound salicylate were determined and were compared to the ratio obtained in solution to determine the degree of binding of salicylate to the entrapped protein relative to solution.

Quenching Studies. Acrylamide and iodide were used to quench the Trp residue in HSA. Samples were placed into a quartz cuvette containing 1.5 mL of PBS, and the sample was titrated with 8.0 M acrylamide or 6.0 M potassium iodide in PBS and allowed to equilibrate for 1 day before measurements were done. Longer equilibration times did not produce any further quenching for the samples. Fluorescence lifetimes were collected in the presence of varying levels of acrylamide or iodide and were converted to intensity weighted mean lifetimes using eq 4. The quenching data was fit using a modified version of the Stern−Volmer equation which accounted for the possibility of there being a fraction of protein that was not accessible to the quencher (f_i):[21,22]

$$\frac{\langle\tau\rangle_0(1 - f_i)}{\langle\tau\rangle - f_i\langle\tau\rangle_0} = 1 + K_{SV}[Q] = 1 + k_q\langle\tau\rangle_0[Q] \quad (6)$$

Here $\langle\tau\rangle_0$ is the intensity-weighted mean lifetime in absence of quencher, $\langle\tau\rangle$ is the intensity-weighted mean lifetime in the presence of quencher, [Q] is the molar concentration of the

(17) Lakowicz, J. R. *Principles of Fluorescence Spectroscopy*, 2nd ed.; Kluwer Academic/Plenum Press: New York, 1999.

(18) James, D. R.; Siemiarczuk, A.; Ware, W. R. *Rev. Sci. Instrum.* **1992**, *63*, 1710. (b) Brennan, J. D.; Flora, K. K.; Bendiak, G. N.; Baker, G. A.; Kane, M.;. Pandey S.; Bright, F. V. *J. Phys. Chem. B* **2000**, *104*, 10100.

(19) O'Connor, D. V.; Phillips, D. *Time-Correlated Single Photon Counting*; Academic Press: Orlando, FL, 1984.

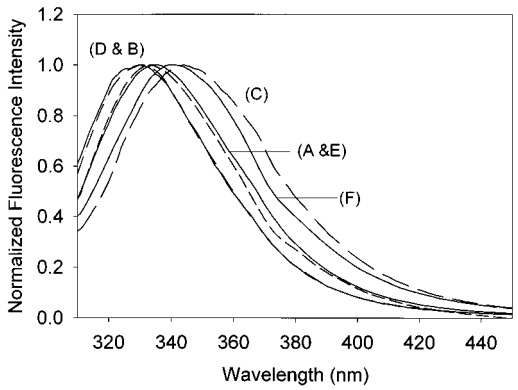

Figure 1. Emission spectra of native and denatured HSA in solution (broken lines) and entrapped in a dry-aged silica monolith (solid lines) after 1 and 24 days of aging: (A) HSA in buffer; (B) HSA in 1.5 M GdHCl; (C) HSA in 4.0 M GdHCl; (D) entrapped HSA, 1 day old; (E) entrapped HSA, 24 days old; (F) entrapped HSA, 24 days old, with 4.0 M GdHCl.

quencher, K_{SV} is the Stern−Volmer quenching constant for the collisional process (M^{-1}), and k_q is the bimolecular quenching constant ($M^{-1}s^{-1}$).

Results and Discussion

Fluorescence Measurements from Entrapped Proteins. Figure 1 shows emission spectra of free (broken lines) and entrapped (solid lines) HSA after 1 and 24 days of aging in dry-aged blocks, along with emission spectra of free HSA in 1.5 and 4.0 M GdHCl (corresponding to partially and fully unfolded HSA, respectively) and the emission spectrum of entrapped HSA in 4.0 M GdHCl after 24 days of aging. In all cases, high-quality emission spectra of the entrapped proteins could be obtained with little or no scattering background from the silica matrix, making for accurate comparisons to the emission spectra of free HSA. The data clearly show that the unfolding of the entrapped HSA can be followed using Trp emission spectra and further indicate that the entrapped HSA can undergo substantial conformational changes, even after 24 days of aging.

Figure 2 shows the decay of tryptophan fluorescence from HSA entrapped into a TEOS-derived matrix that was dry-aged for 24 days, along with the corresponding instrument response function and the residual and autocorrelation plots for a three-component fit (note: $\chi^2_{double} = 1.24$; $\chi^2_{triple} = 0.94$). To our knowledge, this is the first time that the decay of Trp fluorescence has been reported for an entrapped protein, and several points are noteworthy. First, it was not necessary to account for any scattering artifacts from the glass when using sol−gel-derived blocks, with blank glasses providing no significant intensity in the decay curves when sampled at 335 nm. Second, the blank glasses did not alter the polarization of the incident light, indicating that the glass was not birefringent and thus did not

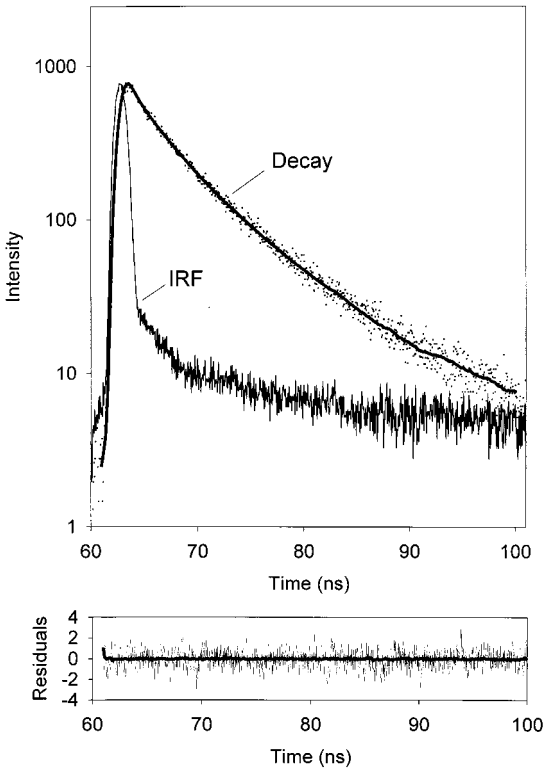

Figure 2. Time-resolved decay of intensity for HSA entrapped in a sol−gel-derived monolith after 24 days of aging and the corresponding instrument response function (IRF). The line shows the best fit through the experimental data for a three-component decay law, along with the corresponding residual (thin line) and autocorrelation (thick line) plots (note: $\chi^2 = 0.94$).

affect the construction of anisotropy decays from the intensity decay data, in agreement with previous reports of anisotropy measurements from sol−gel-entrapped species.[23] Third, the residual and autocorrelation plots indicated that it was possible to fit the decay of tryptophan fluorescence in HSA to three decay components for all samples, in agreement with previous time-resolved fluorescence studies of HSA.[16a,24] Fitting to two components generally resulted in unacceptable χ^2 parameters (>1.20) and nonrandom residual and autocorrelation plots. Fitting to more than three components or to distributions of lifetimes did not improve the fitting statistics. Overall, the good fits to three-component decays indicated that collection and fitting of time-resolved tryptophan emission decay data from entrapped proteins could be done reliably with no background interference from the silica matrix. The ability to fit to discrete decay times also suggests that the protein experiences a single environment rather than a large distribution of environments, consistent with specific protein−silica interactions, as described below.

Conformation and Dynamics. Figure 3 shows the maximum emission wavelengths and steady-state rotational correlation times for free and entrapped HSA as a function of aging time over 2 months. Figure 4 shows the changes in the fractional contributions of the

(20) (a) Demas, J. N. *Excited-State Lifetime Measurements*; Academic Press: New York, 1983. (b) Lakowicz, J. R.; Gryczynski, I. In *Topics in Fluorescence Spectroscopy*; Lakowicz, J. R., Ed.; Plenum: New York, 1991; Vol. 1, Chapter 5. (c) Bright, F. V.; Betts, T. A.; Litwiler, K. S. *CRC Crit. Rev. Anal. Chem.* **1990**, *21*, 389. (d) Bright, F. V. *Appl. Spectrosc.* **1995**, 49, 14A.

(21) Flora, K. K. Brennan, J. D. *Analyst* **1999**, *124*, 1455.

(22) (a) Eftink, M. R.; Ghiron, C. A. *Biochemistry* **1976**, *15*, 672. (b) Eftink, M. R.; Ghiron, C. A. *Biochemistry* **1977**, *16*, 5546. (c) Eftink, M. R.; Ghiron, C. A. *Biochim. Biophys. Acta* **1987**, *916*, 343.

(23) (a) Narang, U.; Wang, R.; Prasad, P. N.; Bright, F. V. *J. Phys. Chem.* **1994**, *98*, 17. (b) Narang, U.; Jordan, J. D.; Bright, F. V.; Prasad, P. N. *J. Phys. Chem.* **1994**, *98*, 8101.

(24) Zolese, G.; Falcioni, G.; Bertoli, E.; Galeazzi, R.; Wozniak, M.; Wypych, Z.; Gratton, E.; Ambrosini, A. *Proteins* **2000**, *40*, 39.

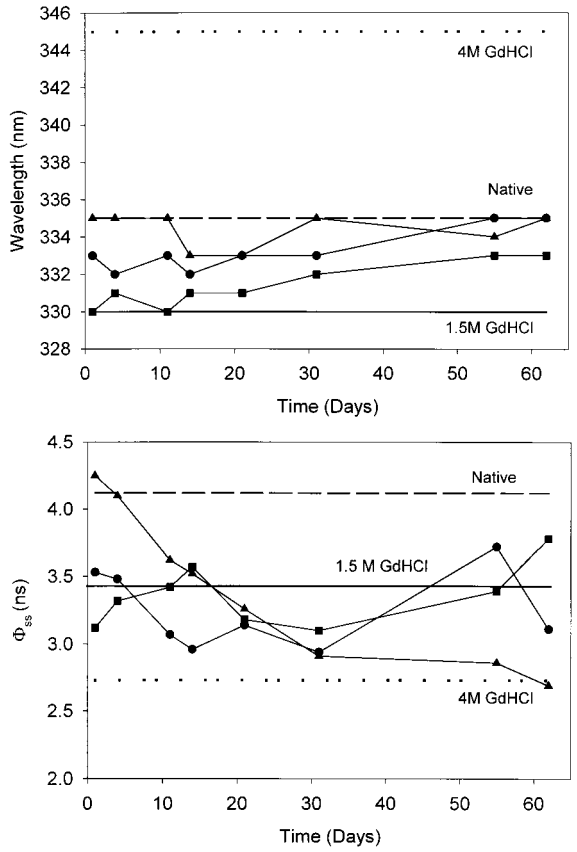

Figure 3. (A) maximum emission wavelength and (B) steady-state rotational correlation times for free and entrapped HSA in dry-aged (■), washed (●), and wet-aged (▲) samples as a function of aging time. The broken line shows the emission wavelength or steady-state rotational correlation time for native HSA in solution. The solid and dotted lines show the emission wavelength and steady-state rotational correlation time for HSA in solutions with 1.5 or 4.0 M GdHCl to provide reference points for partially and fully unfolded HSA. Errors in wavelength values are ±1 nm; errors in correlation times are ±0.1 ns.

three globally linked decay times for entrapped HSA as a function of aging time and condition, along with the mean lifetimes for the entrapped HSA samples during aging over a 2 month period. Spectroscopic studies were terminated at this point as all samples had reached constant mass by this time (25 days for wet-aged samples; 50 days for washed and dry-aged samples) and because all entrapped proteins had lost most of their function by this time (see below). Figures 3 and 4 show that the spectroscopic characteristics of the entrapped protein changed significantly immediately upon entrapment. In general, HSA in dry-aged and washed samples showed a blue-shifted emission maximum, a lower mean lifetime, and a lower rotational reorientation time as compared to HSA in solution (note: for HSA in solution, $\lambda_{em} = 335$ nm, $\langle\tau\rangle = 5.28$ ns, $\phi_{SS} = 4.12$ ns). These results suggested that the protein within dry-aged and washed samples was most similar to free HSA in 1.5 M GdHCl ($\lambda_{em} = 330$ nm, $\langle\tau\rangle = 4.60$ ns, $\phi_{SS} = 3.44$ ns), indicating that the protein may initially adopt an expanded conformation, leading to greater segmental motion for domain II. On the other hand, the emission wavelength and rotational correlation time of HSA in wet-aged samples was initially similar to that in solution, although the mean lifetime was somewhat lower than in solution. This result is consistent with the higher water content within the wet-aged materials, which appears to be able to maintain the protein in a more native-like conformation at early times after entrapment.

As aging continued, the samples evolved somewhat differently depending on the aging method employed. Dry-aged samples tended to show more blue-shifted emission maxima, a significant decrease in the fractional contribution of the long lifetime component with correlated increases in the fraction of the intermediate and shorter lifetime components, lower mean lifetime values, and shorter average rotational reorientation times as aging continued. These results are consistent with the protein adopting a partially expanded form in dry-aged materials. On the other hand, both the washed and wet-aged samples had slightly more red-shifted emission maxima and somewhat longer mean lifetimes than dry-aged samples, suggesting that HSA within such samples, although not in a native conformation, was not as perturbed as HSA in dry-aged samples. Furthermore, the fractional contributions of the various lifetime components remained relatively constant as aging proceeded and only began to decrease slightly at later aging times in washed and wet-aged samples, consistent with smaller conformational changes for HSA in these samples. An interesting point to consider is that even though the steady-state emission spectra of entrapped HSA was often very similar to that of free HSA, the mean lifetimes and steady-state rotational reorientation times were generally quite different for free and entrapped HSA samples, as can be seen from Figures 3 and 4. This result clearly shows the importance of using all aspects of the fluorescence signal to probe protein conformation, since the emission spectrum alone provides only an average of the microenvironments in the region of Trp-214 and, thus, can be misleading.

To further explore protein dynamics, time-resolved anisotropy decay data was obtained for HSA in solution and in each type of glass that had been aged for ~2 months, as shown in Table 1. In all cases, the data for the entrapped protein could be fit relatively well to a hindered rotor model with two rotational components, reflecting local and segmental rotational motions for an adsorbed protein. Fitting to three or more components did not improve the statistics of the fits and generally resulted in two of the three recovered rotational reorientation times having equivalent values. The only cases where relatively poor fits were obtained were for HSA in 2.0 or 4.0 M GdHCl. In these cases, it is likely that the denatured protein adopted a large number of orientations and, therefore, would have required a distribution of reorientation times to fit the anisotropy decay data.

HSA in solution did not show hindered rotation ($r_\infty \approx 0$) and provided two rotational reorientation times of 20 ns (global motion) and 0.44 ns (local motion), with the relative weighting of these motions being 2:1, in good agreement with previous reports.[24] As the protein was denatured in solution, the residual anisotropy remained at a value of zero (no hindered rotational motion), while the global reorientation time decreased initially, likely owing to increased segmental motion for domain II.[16a] Further denaturation led to the proportion of local motion increasing, with a corresponding increase in the

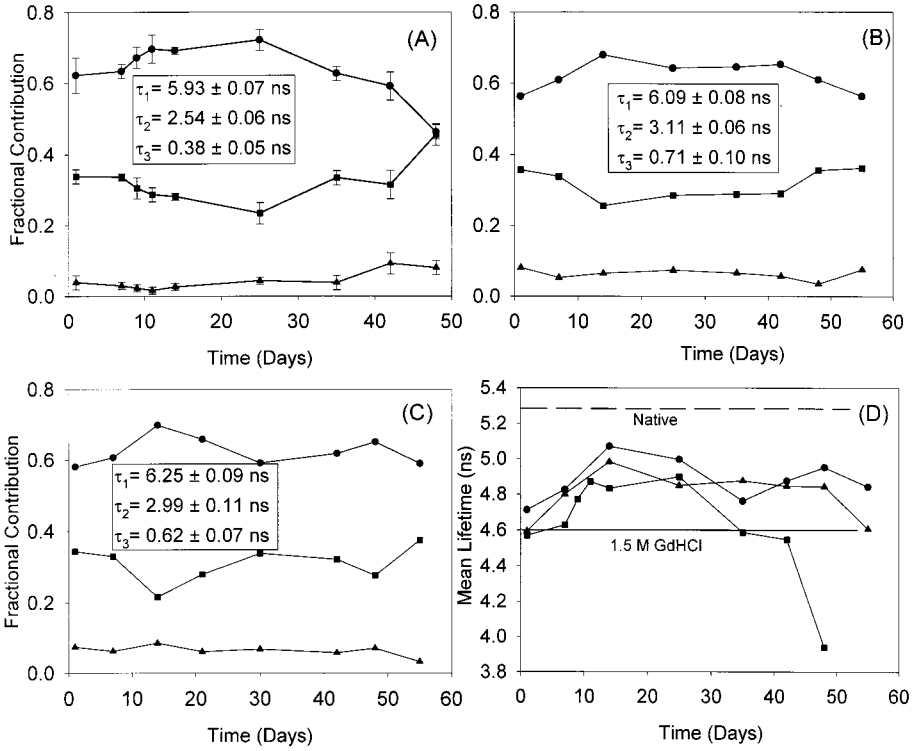

Figure 4. Changes in the fractional contributions of the three globally linked decay times for entrapped HSA in (A) dry-aged (χ^2 = 1.14), (B) washed (χ^2 = 1.19), and (C) wet-aged (χ^2 = 1.20) glasses as a function of aging time. (D) Mean lifetimes for the entrapped HSA samples during aging over a 2-month period, as determined from eq 4, for dry-aged (■), washed (●), and wet-aged (▲) samples. The dashed and solid lines show the mean lifetime for HSA in solutions with 0 or 1.5 M GdHCl to provide reference points for native and partially unfolded HSA. For reference, the mean lifetime of HSA in 4.0 M GdHCl was 2.73 ns. Typical errors for fractional components are shown in panel A. Typical errors for mean lifetimes were ca. ±0.1 ns.

Table 1. Time-Resolved Fluorescence Anisotropy Decay Parameters for Free and Entrapped HSA as a Function of Aging Time

sample	ϕ_1 (ns)[a]	ϕ_2 (ns)	β_1[b]	β_2	r_∞[c]	SSR[d]
			Solution			
native	20.01	0.44	0.67	0.33	0.01	2.551×10^{-6}
1.0 M GdHCl	10.18	0.42	0.69	0.31	0.01	2.638×10^{-6}
2.0 M GdHCl	9.14	0.42	0.82	0.12	0.01	2.863×10^{-5}
4.0 M GdHCl	19.18	0.56	0.38	0.62	0.00	5.617×10^{-5}
35% EtOH	11.75	1.17	0.55	0.45	0.02	6.760×10^{-8}
			Entrapped			
day 1 washed	10.55	1.50	0.15	0.85	0.15	8.129×10^{-7}
day 30 washed	4.81	0.25	0.03	0.97	0.11	8.693×10^{-7}
day 51 washed	4.90	0.29	0.01	0.99	0.11	3.788×10^{-7}
day 1 wet	7.24	1.36	0.38	0.62	0.13	2.864×10^{-7}
day 30 wet	2.61	0.20	0.06	0.94	0.12	2.999×10^{-6}
day 51 wet	3.93	0.20	0.05	0.95	0.13	5.254×10^{-6}
day 1 dry	5.66	0.35	0.37	0.63	0.13	9.113×10^{-7}
day 30 dry	5.62	1.23	0.14	0.86	0.12	7.512×10^{-8}
day 51 dry	10.39	1.83	0.44	0.56	0.14	2.685×10^{-7}

[a] Typical error in rotational correlation times is ±2%. [b] Typical error in fractional contributions of anisotropy decay times is ±0.01. [c] Typical errors in r_∞ values are ±0.01. [d] Sum-of-squares of residuals between line of best fit and experimental data.

global and local reorientation time, likely signifying unfolding to a molten globule, with a solvent exposed Trp residue now rotating with the whole protein rather than an individual domain.

Upon entrapment of HSA, the most striking change in the anisotropy decay was the high value of the residual anisotropy (r_∞ > 0.11 in all cases). This large residual anisotropy value is consistent with adsorption of the probe onto the surface of the glass, causing a restriction in the global rotational motion of the protein. A second unexpected result was that the value of the longer rotational reorientation time *decreased* from 20 ns to between 5.6 and 10.5 ns, and the proportion of the short rotational component increased, consistent with greater mobility in the region of Trp-214 (in agreement with the steady-state reorientation time values shown in Figure 3). Given that many studies have conclusively demonstrated a higher internal microviscosity for solvents within sol−gel-derived glasses (which argues against faster overall rotational motion for the protein),[11] the increase in the rotational correlation time of the protein in the region of Trp-214 is most likely due partial unfolding of the protein, leading to independent motion of domain II, which is known to dissociate from domains I and III under mildly denaturing conditions.[16a]

As aging proceeded, considerable differences could be seen in the rotational reorientation times, depending on the aging method employed. For the washed and wet-aged samples, both the segmental and local reorientational times decreased, and the proportion of local motion increased. These results are consistent with unfolding of the protein in the region of Trp-214, which would result in exposure of the Trp residue to solution and a higher degree of local bond rotation. Hence, the anisotropy data confirm that local conformational changes consistent with protein unfolding occur as aging progresses. At later aging times the segmental reorientation times appear to increase slightly (as do the steady-state reorientation times), likely due to increased local microviscosity as the pores shrink.[11]

In the case of the dry-aged sample, the anisotropy data evolved somewhat differently, with an increase in both the segmental and local reorientation times at longer aging times (in agreement with the steady-state reorientation times), suggesting a higher overall microviscosity for the entrapped solvent. A key observation is that, in all cases, the reorientation times are consistent with partially unfolded protein and *do not* reflect a complete loss of mobility, owing to the retention of local segmental motion in domain II of the protein. The retention of motion within domain II for entrapped HSA indicates that the protein likely adsorbs in an orientation that results in exposure of this domain to the pore solvent. This is consistent with expectations given that both domain II and the silicate are negatively charged at pH 7.2[10,14,15] and, thus, would be electrostatically repelled. Our results also agree qualitatively with those of Bright et al.,[3a] who also observed retention of mobility for domain I of entrapped HSA labeled with acrylodan at Cys-34. Furthermore, the adsorption of the protein to the glass (likely through domain III on the basis of our results and those of Bright et al.[3a]) is consistent with the results obtained by Friedman and co-workers for myoglobin[3b] and by Bright et al. for the anti-dansyl antibody,[3c] which showed these entrapped proteins to be essentially immobile after aging of TEOS-derived glasses. These latter results have been interpreted in terms of electrostatic interactions between the protein and silicate at neutral pH[3b,25] or in terms of templating of the silicate around a relatively rigid protein,[3c] leading to little or no segmental motion and, thus, very slow tumbling within the glass owing to the higher microviscosity of the internal solvent.

On the basis of the steady-state and time-resolved fluorescence data, it is clear that human serum albumin adsorbs to the glass and undergoes substantial changes in conformation in the region of Trp-214 upon entrapment, which likely reflect a shift from the native to the expanded form of the protein.[16a] Electrostatic interactions of HSA with surfaces and ions, and resulting changes in protein conformation, have been widely reported before,[26] and thus, it is likely that association

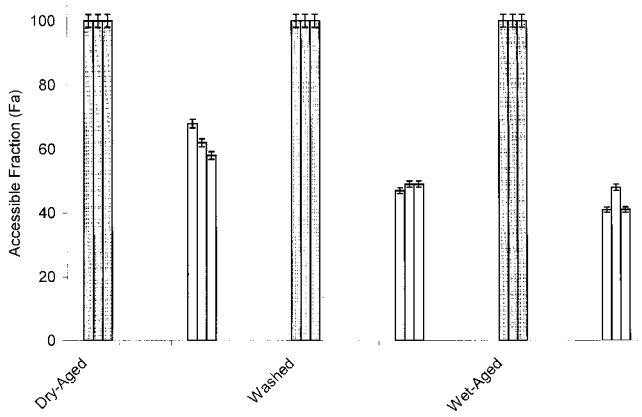

Figure 5. Fractional accessibility of entrapped HSA to fluorescence quenchers. Shaded bars refer to acrylamide, and open bars refer to iodide. The first bar in each set represents day 1 of aging, the middle bar is day 30, and the last bar in each set is day 62.

of HSA with the negatively charged silicate surface was at least partially responsible for the significant conformational changes in the protein. As aging continues, the local mobility of the Trp residue increases, and a small red-shift is observed (for dry-aged and washed samples), consistent with partial unfolding of domain II. Most importantly, it was not possible to maintain the protein in a native conformation using *any* of the three aging methods, suggesting that HSA−surface interactions with the polar, anionic silica matrix caused the relatively "soft" HSA molecule to be susceptible to unfolding when entrapped, regardless of the aging method employed.

Accessibility. Figure 5 shows the fractional accessibility values for acrylamide and iodide quenching of entrapped HSA on days 1, 30, and 62 for each type of aging condition (note: free HSA was fully accessible to both quenchers at all times). Acrylamide was used as it is neutral and thus avoids electrostatic contributions to accessibility. Iodide was used since it mimics the electrostatic behavior of the analyte, salicylate, which is used below for determination of the degree of ligand binding to entrapped HSA. The acrylamide quenching data for all samples could be fit well without having to incorporate a correction for an inaccessible fraction of protein (i.e., all protein was accessible to the neutral quencher at all times). However, in the case of iodide, all samples showed significant decreases in fractional accessibility, with the amount of accessible protein ranging from 41% to 68% of that in solution, in agreement with previous studies by Saavedra et al.[2c,4] Given that both iodide and the silicate matrix are negatively charged at neutral pH, it is perhaps not surprising that the anionic quencher was unable to penetrate into all regions of the matrix. However, to our knowledge, this is the first time that electrostatic interactions have been directly demonstrated as a cause of analyte inaccessibility to entrapped proteins. These results suggest that analyte−matrix and protein−matrix interactions need to be carefully considered in the design of sol−gel-based biosensors for charged analytes.

Thermal Stability. Figure 6 shows typical fluorescence-based thermal unfolding curves generated for free and entrapped HSA that had been aged for 11 days in

(25) (a) Chen, Q.; Kenausis, G. L.; Heller, A. *J. Am. Chem. Soc.* **1998**, *120*, 4582−4585. (b) Heller, J.; Heller, A. *J. Am. Chem. Soc.* **1998**, *120*, 4586−4590.

(26) (a) Guillaume, Y. C.; Guinchard, C.; Robert, J. F.; Berthelot, A.; *Chromatographia* **2000**, *52*, 575. (b) Taboada, P.; Mosquera, V.; Ruso, J. M.; Sarmiento, F.; Jones, M. N. *Langmuir* **2000**, *16*, 6795. (c) Trynda-Lemiesz, L.; Karaczyn, A.; Keppler, B. K.; Kozlowski, H. *J. Inorg. Biochem.* **2000**, *78*, 341. (d) Purcell, M.; Neault, J. F.; Tajmir-Riahi, H. A. *Biochim. Biophys. Acta* **2000**, *1478*, 61.

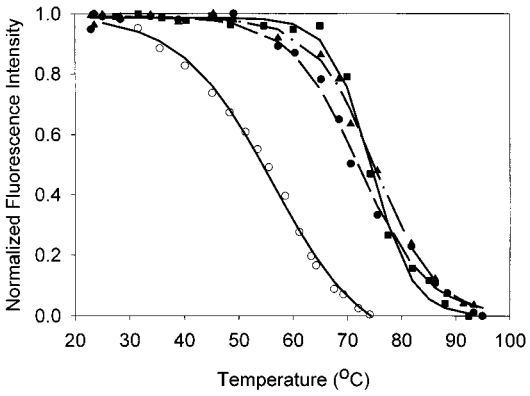

Figure 6. Fluorescence-based thermal unfolding curves generated for free HSA (○) and for entrapped HSA that had been aged for 11 days in glasses that were dry-aged (experimental points, ■; fit line, —), washed (experimental points, ●; fit line, – –), and wet-aged (experimental points, ▲; fit line, – • –).

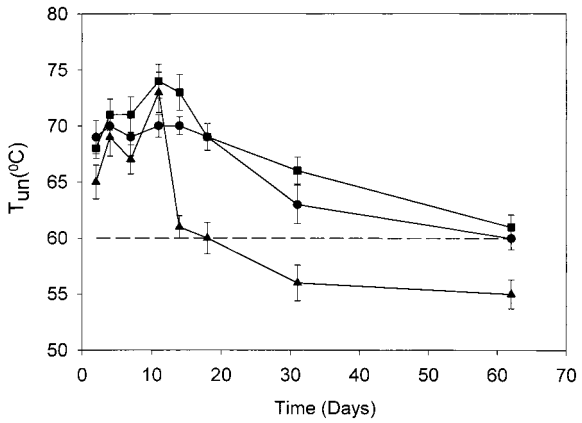

Figure 7. Unfolding temperatures calculated for free HSA (broken line) and for entrapped HSA in dry-aged (■), washed (●), and wet-aged (▲) samples as a function of sample aging.

dry-aged, washed, and wet-aged blocks. Figure 7 shows the unfolding temperatures calculated for free and entrapped HSA samples as a function of sample aging. The unfolding transitions were observed to be irreversible, in agreement with the results obtained for HSA in solution;[16a] thus, it was not possible to determine thermodynamic parameters for protein unfolding. It is clear that the unfolding temperature of the protein increases significantly upon entrapment, regardless of the aging method employed. This effect has been reported previously in several papers[2b,8,9,27] and is thought to be the result of molecular confinement.[27] However, the electrostatics in the vicinity of the entrapped protein may also play a role in the stabilization, as high levels of anions have been observed to stabilize HSA in solution.[28]

As aging proceeds, the apparent unfolding temperature decreases for all samples, likely reflecting the fact that the initial conformation of the entrapped protein is significantly different than in solution, producing a less stable form of the protein. It should also be noted that the data in Figure 1 (spectra C and F) suggest that the final state of the protein may also be different upon entrapment (at least for dry-aged samples). This conclusion is based on the blue-shifted emission maximum of the entrapped protein in 4.0 M GdHCl as compared to the free protein with this level of denaturant, reflecting incomplete unfolding of HSA in the glass.[2b,8,9] The apparent increase in the thermal unfolding temperature of the entrapped proteins at early aging times, coupled with the spectroscopic evidence for incomplete unfolding, is consistent with previous reports,[2b,8,9,27] and suggests that the internal environment of the sol–gel-derived glass is able to restrict large-scale conformational changes in the protein. This result suggests that the unfolding temperatures are likely only approximate indicators of overall stability, as they do not reflect unfolding from a fully native conformation to a fully unfolded state, as is the case in solution. Furthermore, our results suggest that the increased unfolding temperatures are transient, as the unfolding temperature eventually decreases to a value equal or lower than that of the protein in solution. Hence, it is clear that entrapment of the protein will not necessarily lead to an improvement in long-term thermal stability.

Salicylate Binding. While studies of conformation, dynamics, and thermodynamic stability can provide insight into how entrapment alters protein structure and mobility, the most critical parameter that determines the success of a particular entrapment protocol is the degree of ligand binding retained by the entrapped biomolecule. We therefore examined the ability of free and entrapped HSA to bind to the model fluorescent ligand salicylate. The free form of salicylate fluoresces with an emission maximum at 408 nm, and upon binding of salicylate to domain II of HSA, the fluorescence intensity and mean lifetime both increase with a corresponding decrease in Trp emission intensity owing to Trp-to-salicylate fluorescence energy transfer. It was found that emission intensity results could not be used reliably to ascertain the ability of ligand to bind entrapped HSA, owing to difficulties encountered with reproducible mounting of samples, which led to problems related to proper subtraction of appropriate blanks. Fluorescence decay data is insensitive to sample concentration and, thus, is unaffected by small differences in positioning of samples in the instrument. For this reason, all salicylate binding data were obtained using fluorescence lifetime analysis of salicylate in the absence of HSA and with a molar ratio of 1.75:1.00 of salicylate:HSA. Free salicylate showed a single decay time of 4.1 ns (both in solution and in glasses that contained no HSA), while the complex of salicylate with free or entrapped HSA had a biexponential decay with a 4.1 ns component (free salicylate) and a 9.0 ns component (bound salicylate). Denaturation of the complex led to the recovery a single decay time of 4.1 ns, confirming that the longer lifetime component was due to bound salicylate. By comparison of the preexponential (α_i) values of the two lifetime components, it was possible to determine the relative degree of salicylate binding to entrapped HSA as compared to free HSA. For example, binding of salicylate to free HSA resulted in a preexponential factor of 0.38 for the long component, while the long component for salicylate:HSA in a 2 day old wet-aged monolith had a fractional contribution of only 0.23, or 60% that of solution. This is interpreted as being due to binding of 60% of the amount of salicylate that was bound by free HSA.

(27) Eggers, D. K.; Valentine, J. S. *Protein Sci.* **2001**, *10*, 250.
(28) Muzammil, S.; Kuman, Y.; Tayyab, S. *Proteins* **2000**, *40*, 29.

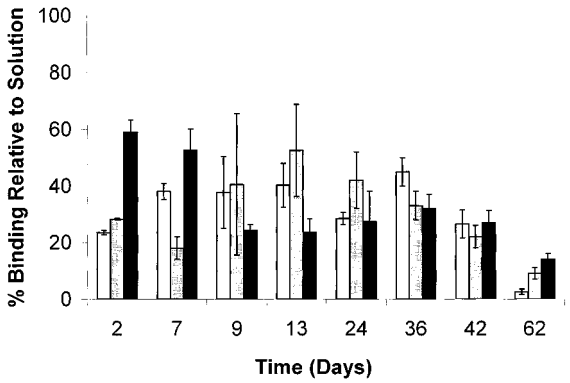

Figure 8. Percent of ligand binding retained vs solution for HSA entrapped in wet-aged (open), washed (hatched), and dry-aged (solid) monoliths as a function of aging time.

Figure 8 shows the fraction of retained ligand binding for HSA entrapped in dry-aged, washed, and wet-aged monoliths as a function of aging time. In all cases and for all aging times the degree of salicylate binding was between 5% and 60% of the value in solution; i.e., no samples showed full retention or complete loss of ability to bind ligand as compared to free HSA. Surprisingly, dry-aged samples initially showed the highest retention of ligand binding ability, with almost 60% of the binding observed in solution as compared to about 25% binding for washed and wet-aged samples. As aging continued, the percentage of functional protein in dry-aged samples decreased steadily, dropping to about 15% by day 65. Given that the accessibility of the protein to iodide remained relatively constant over this period, the loss of ability to bind ligand is likely due to denaturation of the protein over time, in agreement with the spectroscopic data presented in Figures 1−4.

Both washed and wet-aged samples evolved somewhat similarly to each other but quite differently from dry-aged samples. In both cases, the entrapped protein initially showed significantly lower binding ability as compared to dry-aged samples, perhaps reflecting the somewhat lower accessibility to charged analytes found for these samples and/or differences in the ligand binding constant of HSA, which is known to be affected by changes in electrostatics and ionic strength.[26] However, by day 13 both samples reached a maximum in relative ligand binding ability, suggesting that all accessible protein was functional at this point. Beyond the 13th day of aging, both washed and wet-aged samples slowly decreased in binding ability, corresponding to the decreases in unfolding temperature and the changes in spectroscopic parameters beyond this point. These results suggest that slow denaturation of the protein begins at this point and continues over the entire period of aging, in agreement with spectroscopic data on the entrapped protein.

It is known that the unfolding of HSA occurs by a multistep process involving separation of domain II from domains I and III, followed by unfolding of domain II, and finally unfolding of domains I and III.[16a] The initial domain separation step can be achieved with ∼1.5 M GdHCl and produces spectroscopic signatures similar to those of entrapped HSA at early aging times. This step also reduces that ability of the protein to bind salicylate,[16a] and hence, the spectroscopic evidence suggests that the loss of salicylate binding ability may be correlated to the expansion of the protein structure. Thus, the overall picture that emerges is one wherein the ability to bind a ligand is controlled by accessibility at early aging times and by protein denaturation at longer times. It is also clear that no aging method is able to retain the entrapped protein in a functional state when using materials derived from pure TEOS, suggesting that alternative sol−gel processing methods (such as inclusion of organosilane precursors, polymers, or other additives) will be needed to control protein−surface interactions and, thus, provide improved stability for entrapped proteins.

Conclusions

On the basis of the spectroscopic data presented herein, it is clear that the entrapment of human serum albumin into TEOS-based glasses results in significant changes in protein behavior, regardless of the aging method employed. Immediately upon entrapment, it appears that the protein undergoes a conformational change consistent with an expansion of the protein structure and that the protein adsorbs to the silica surfaces within the pores, resulting in hindered rotational mobility. The conformation of the protein continues to change slowly as the silica matrix evolves, eventually reaching a partially unfolded state that shows little ability to bind to ligands. The conformational changes in the entrapped protein suggest that much of the protein likely resides in pores that have sufficient free volume to permit at least partial unfolding of the protein, although there is evidence that full unfolding of the protein is restricted, likely owing to templating of the sol−gel matrix around the protein during entrapment.

The entrapment of HSA into TEOS-derived glasses also leads to significant decreases in the amount of protein that is accessible to anionic species. On the other hand, the protein remains fully accessible to uncharged species, even after 2 months of aging, suggesting that electrostatic interactions play a major role in determining the penetration of analytes into the sol−gel matrix. This result indicates that analyte−matrix and protein−matrix interactions must be carefully controlled in cases where sol−gel-based biosensors are used for sensing of anionic analytes.

In general, HSA showed significant losses in ligand binding ability in all glasses, regardless of the aging method used. Our results suggest that the lower degree of ligand binding is due to both partial inaccessibility to anionic analytes (which was predominant at early aging times) and partial denaturation of the entrapped protein (which was more important at later aging times). Wet-aged samples provided the highest retention of function over the first month of aging, suggesting that this aging method may be useful in cases where long-term storage of the entrapped protein is not required. However, all entrapped proteins showed retention of 15% or less of their binding capacity in solution after 2 months of aging, clearly demonstrating that the aging method can only maintain proteins in a functional state over relatively short periods. Overall, the results indicate that TEOS-based bioglasses are not likely to be amenable to commercial applications, owing to long-term alterations in protein conformation and ligand

binding. On the basis of these finding, it is clear that the development of new sol−gel processing methods (using different precursors, additives, and/or aging methods) will be necessary to produce "second-generation" glasses that are able to stabilize proteins in an active form.

Acknowledgment. The authors thank the Natural Sciences and Engineering Research Council of Canada, MDS-Sciex, and MDS Proteomics for financial support of this work.

CM010155L